Thermoelectric power and electrical conductivity of amorphous Au_xSb_{100-x} films near the metal-insulator transition

1995 J. Phys.: Condens. Matter 7 1305

(http://iopscience.iop.org/0953-8984/7/7/012)

J. Phys.: Condens. Matter 7 (1995) 1305–1314. Printed in the UK

Thermoelectric power and electrical conductivity of amorphous Au_xSb_{100-x} films near the metal–insulator transition

C Lauinger† and F Baumann

Physikalisches Institut, Universität Karlsruhe, 76128 Karlsruhe, Germany

Received 27 October 1994

Abstract. The thermoelectric power S and the electrical conductivity σ of amorphous Au_xSb_{100-x} films have been investigated in the temperature range between about 5 K and 350 K. A detailed experimental investigation is performed near the metal–insulator transition occurring at $x_c = 8.1$ at.% Au. For $x_c < x < 16.8$ at.% the extrapolated values of $\sigma(0)$ show a scaling behaviour with a critical exponent $\nu \simeq 1$. In the same concentration range the low-temperature slope of the diffusion thermopower S_D, i.e. $S_D(T)/T\,|_{T\to 0}$, increases very rapidly for samples approaching x_c. A linear correlation between $S_D(T)/T\,|_{T\to 0}$ and $1/\sigma(0)$ is found which is interpreted in terms of a non-interacting electron system showing an Anderson transition.

1. Introduction

It has been known for some years that pure Sb films can be prepared in an amorphous non-metallic phase [1, 2]. Crystallization occurs during annealing at about 280 K. The conductivity σ shows variable-range hopping according to Mott's law for $T < 100$ K [3]. Quench-condensed Au_xSb_{100-x} films which are amorphous up to $x < 80$ at.% [4, 5] show a metal–insulator (MI) transition at a critical concentration $x_c \simeq 8$ at.% Au [6]. In the metallic region amorphous Au_xSb_{100-x} films are superconducting with a maximum transition temperature $T_c \simeq 3$ K at about 40 at.% Au [4].

The purpose of this investigation is twofold. One reason is to look for a correlation between the thermopower and the resistivity approaching the MI transition in the metallic region. Comparing experimental results with theoretical predictions should give information about the kind of the transition as well as about the influence of the electron–electron interaction in this highly disordered material. Another reason is that we need the knowledge of the thermopower of amorphous Au_xSb_{100-x} films in order to be able to discuss our recent results on Au/Sb sandwiches [7, 8]. The transport properties of ultrathin Au films on top of amorphous Sb films indicate that these Au/Sb sandwiches behave like amorphous Au_xSb_{100-x} alloys.

For these reasons we report in this paper on S and σ of amorphous Au_xSb_{100-x} films with $x < 80$ at.% but focus our interest on the metallic region near the MI transition.

† Present address: Institut für Physik, TU Chemnitz-Zwickau, 09107 Chemnitz, Germany.

0953-8984/95/071305+10$19.50

2. Experimental details

The *in situ* measurements of the thermopower and the electrical conductivity were performed in a ^{4}He cryostat in the temperature range between about 5 K and 350 K. The reference material in the thermocouple was a cold-rolled 99.9999% Pb foil with a thickness $d_{Pb} \simeq 40-50\,\mu$m which was glued onto the glass substrate before mounting all the equipment into the cryostat. With the absolute thermopower of Pb known, the absolute thermopower of the sample investigated can be determined. Our calibration data on the thermopower of the lead foil against a superconducting Nb_3Sn wire agree very well with the generally accepted data of Roberts [9] except for as regards small deviations of the order of 10 nV K^{-1} at 15 K. These deviations are probably due to the different treatments of the Pb reference. The thermopower was measured using a dynamical method which allows one to take data above 4 K. This method as well as the sample preparation are described elsewhere [10]. The conductivity σ was measured using a standard four-wire DC technique and the data were taken above 1.7 K.

The amorphous Au_xSb_{100-x} films were obtained by flash evaporation of small portions of the alloy onto a glass substrate held at liquid He temperature. During the evaporation the pressure in the cryostat rose from about 3×10^{-8} mbar to approximately 5×10^{-7} mbar. The thickness of the films which varied between about 1000 Å and 4000 Å was controlled using a quartz thickness monitor. The typical deposition rate was approximately 2 Å s^{-1}. During the deposition procedure the temperature of the sample holder increases to about 20 K. Using this method one obtains homogeneous amorphous Au_xSb_{100-x} films for $0 \leqslant x \leqslant 80$ at.% [4, 5]. After the condensation process the samples were annealed step by step up to a temperature of 350 K, which is well above the crystallization temperature of the samples [4]. Besides the reversible temperature dependences of S and σ, we have also measured both quantities during annealing to get information about irreversible changes of the samples.

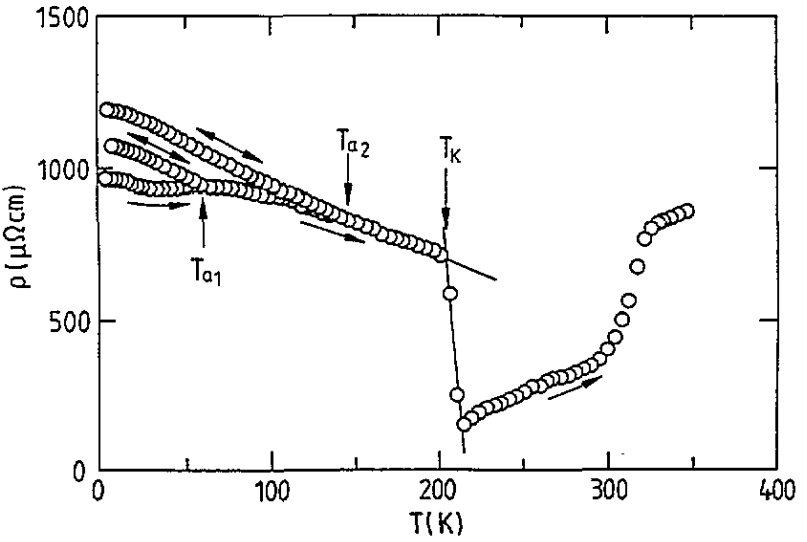

Figure 1. Temperature dependence of the electrical resistivity ρ of a $Au_{12.2}Sb_{87.8}$ film. $\longleftrightarrow$ reversible changes; $\longrightarrow$ irreversible changes; T_K crystallization temperature. The film was annealed at $T_{a_1} = 60$ K and $T_{a_2} = 185$ K.

3. Results and discussion

3.1. Electrical resisitivity

Figure 1 shows the resistivity ρ of a $Au_{12.2}Sb_{87.8}$ film versus the temperature. After the first annealing at about 60 K the resistivity has increased slightly. Further annealing results in an additional irreversible increase of ρ. At the temperature T_K ρ shows a strong decrease due to the crystallization of the sample. The values for T_K are qualitatively in good agreement with the results given in [4], but are shifted to smaller values due to an improved sample preparation technique. The annealing behaviour in the amorphous state shown in figure 1 is typical for all metallic films with $x < 20$ at.%. The irreversible increase of the resistivity is the more pronounced the lower the Au content. A quite similar annealing behaviour was observed in case of amorphous Au_xSi_{100-x} [11] and Au_xGe_{100-x} films [12]. It was explained as being due to segregation effects. This explanation was also supported by UPS measurements on amorphous AuSi [11]. In order to avoid such inhomogeneities as far as possible we focus our interest in this paper on amorphous films with a maximum annealing temperature of about 60 K. Films with $x > 20$ at.% show a different annealing behaviour. Their resistivity decreases slightly during annealing.

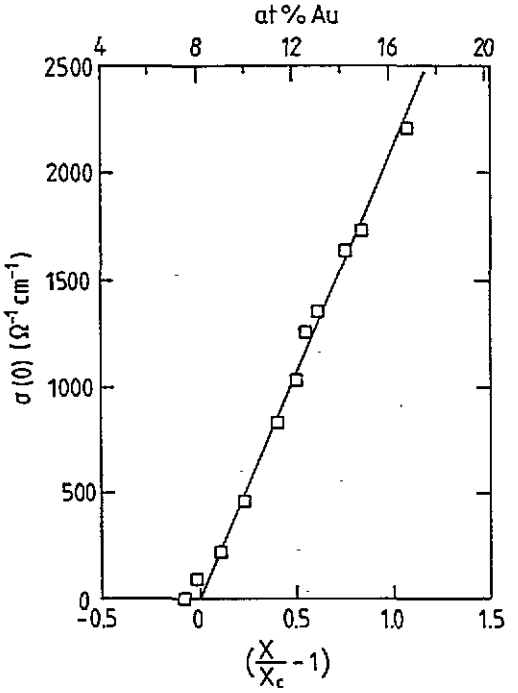

Figure 2. Electrical conductivity $\sigma(0)$ extrapolated to $T = 0$ K as a function of the Au concentration near the critical concentration x_c.

Figure 2 shows the concentration dependence of the conductivity $\sigma(0)$ extrapolated to $T = 0$ for the films with $x < 20$ at.%. $\sigma(0)$ was determined through linear extrapolation of the data above about 1.7 K and was taken after the films were annealed at 60 K. The uncertainties in the values of $\sigma(0)$ are largest in the case of Au_9Sb_{91} and are estimated to be about 1%. For this film the relative increase of the resistivity between 2 K and 10 K is approximately 5%, in the case of $Au_{11.4}Sb_{88.6}$ it is only 0.1%. The $T^{1/2}$-dependence of the

resistivity at lowest temperatures due to weak localization and electron–electron interaction in the metallic region near the MI transition which was observed in other amorphous systems, e.g. Nb_xSi_{100-x} [13], was masked by superconducting fluctuations.

The data shown in figure 2 can be described by $\sigma(0) = \sigma_0(x/x_c - 1)^\nu$ for $x \geqslant x_c$ with a critical exponent $\nu = 1.15 \pm 0.1$ which is close to 1. A scaling behaviour with $\nu = 1$ is expected for a three-dimensional non-interacting electron system showing a disorder-driven MI transition, i.e. an Anderson transition [14]. The value $\nu \simeq 1$ is typical for amorphous systems and compensated semiconductors and has also been observed, e.g., in amorphous Nb_xSi_{100-x} [13] and amorphous Bi_xKr_{100-x} [15]. In addition the critical Au concentration can be determined from figure 2 to be $x_c = (8.1 \pm 0.1)$ at.%, which is in good agreement with an earlier investigation [6]. The constant σ_0 is $(2061 \pm 40)\ \Omega^{-1}\ cm^{-1}$.

For a $Au_{7.5}Sb_{92.5}$ film with a concentration just below x_c $\sigma(T)$ shows variable-range hopping according to Mott's law [16]

$$\sigma(T) \propto \exp(-(T_0/T)^{1/4}) \tag{1}$$

for $T < 25$ K. The temperature-independent parameter T_0 is about 1.3×10^4 K.

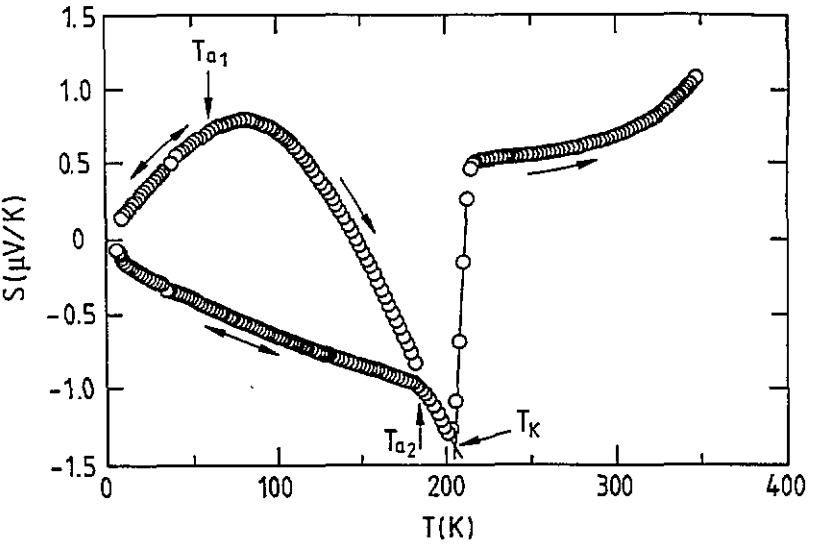

Figure 3. Temperature dependence of the thermopower S of a $Au_{12.2}Sb_{87.8}$ film. Notation as in figure 1.

3.2. Thermoelectric power

Figure 3 shows the annealing behaviour of the thermopower S for a film with $x = 12.2$ at.% Au. This is the same sample for which $\rho(T)$ was shown in figure 1. For all the films investigated annealing below 60 K has only little effect on the thermopower. Very pronounced irreversible changes in $S(T)$ which occur during annealing above 60 K are restricted to films with $x < 20$ at.%. The changes increase with decreasing x. A characteristic feature is a maximum in $S(T)$ between 80 K and 100 K, which appears at higher temperatures for films with lower x. The height of the maximum increases with decreasing x. After annealing just below the crystallization temperature $S(T)$ has changed its sign, now being negative and nearly independent of x. Only a sample with x close to

x_c did not change the sign of $S(T)$ during annealing. Amorphous films with $x > 40$ at.% show no irreversible changes in S or σ below the crystallization temperature. In order to exclude segregation effects which may be responsible for these changes, all data shown in the following figures are taken for amorphous films annealed up to 60 K.

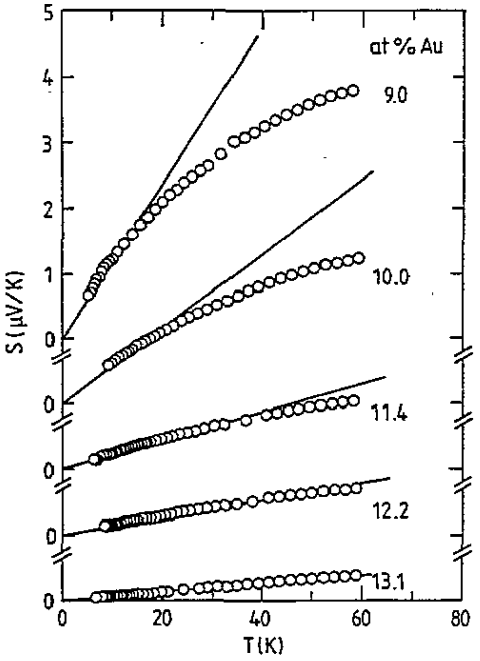

Figure 4. Thermopower S of amorphous Au_xSb_{100-x} in the vicinity of x_c after annealing at 60 K. The numbers next to the data give the Au content in at.%. The straight lines are calculated using linear regression.

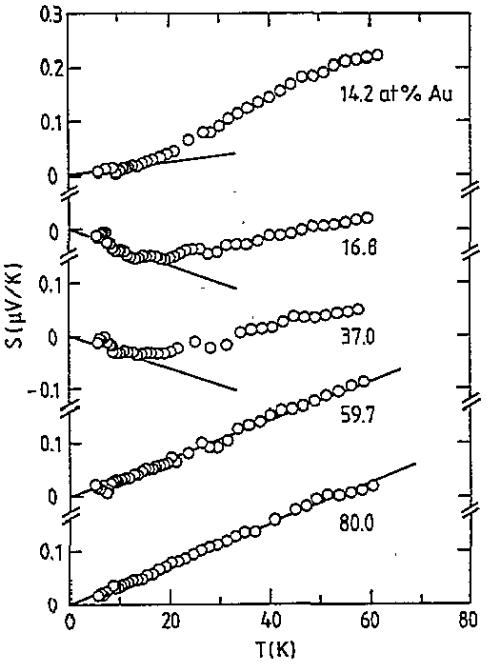

Figure 5. Thermopower S of amorphous Au_xSb_{100-x} for $x \geqslant 14.2$ at.% after annealing at 60 K. The numbers next to the data give the Au content in at.%. The straight lines are calculated using linear regression.

Figures 4 and 5 give an overview of the reversible part of $S(T)$ for $T < 60$ K and $x > x_c$. The solid lines are calculated from the low-temperature data using linear regression under the condition $S \to 0$ for $T \to 0$ which necessarily has to be fulfilled in the case of metals. The slope calculated in this way yields the slope of the measured $S(T)$ in the limit $T \to 0$, i.e. $S/T|_{T\to 0}$. The concentration dependence of $S/T|_{T\to 0}$ is summarized in figure 6. Approaching the critical concentration x_c there is a remarkable increase in the slope of the low-temperature thermopower. On the other hand, for 60 at.% $\leqslant x \leqslant$ 80 at.% the slope of S is independent of x and positive and approximately a factor of 1/2 smaller than the value which is measured on a quench condensed and microcrystalline Au film ($d_{Au} \simeq 600$ Å) for which $S/T|_{T\to 0} \simeq 8$ nV K^{-2}. Between 16.8 at.% $< x <$ 37 at.% $S/T|_{T\to 0}$ *is negative. This is connected with a dip in* $S(T)$ *between about 10 K and 20 K* (see figure 5) which is, in our opinion, due to virtual electron–phonon interaction and which is most pronounced in the concentration range where the samples are superconducting.

The very rapid increase of the thermopower in the vicinity of the MI transition has to be compared with theoretical predictions in terms of the diffusion thermopower $S_D(T)$. For this reason additional contributions $S_{add}(T)$ caused by virtual electron–phonon interaction

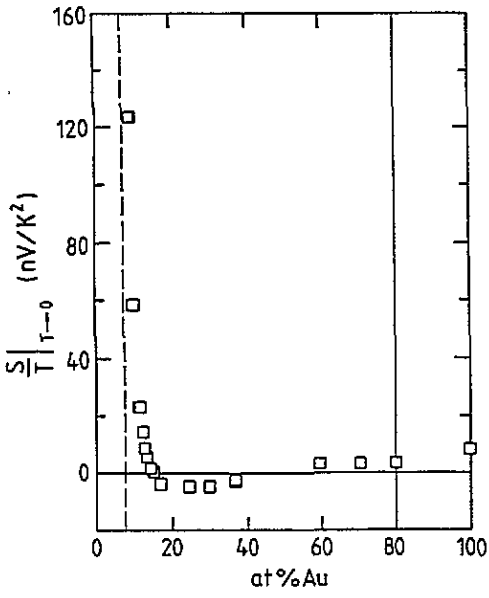

Figure 6. Concentration dependence of $S/T|_{T\to 0}$ of amorphous Au_xSb_{100-x} above x_c. The values were measured after annealing at 60 K. The vertical solid line gives the upper limit of the amorphous range. The vertical dotted line gives the position of x_c.

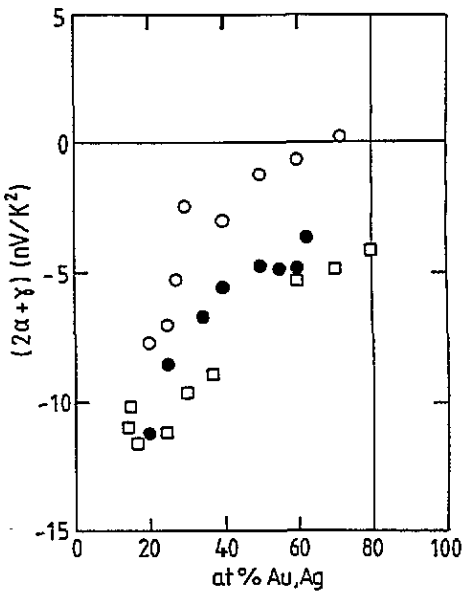

Figure 7. $[2\alpha + \gamma]$ as a function of the noble-metal content for different amorphous alloys. □, Au_xSb_{100-x} (this work); ○, Au_xSn_{100-x} [26]; ●, Ag_xIn_{100-x} [26]. The vertical solid line marks the upper limit of the amorphous range of AuSb.

have to be subtracted from the thermopower $S(T)$ we have measured. According to Kaiser [17] and Kaiser and Stedman [18] $S(T)$ is given by

$$S(T) = S_D(T) + S_{add}(T) \qquad \text{with} \qquad S_{add}(T) = \left[\frac{S_D(T)}{T} + 2\alpha + \gamma\right] T\,\lambda(T) \tag{2}$$

which is the same as

$$S(T) = [1 + \lambda(T)]S_D(T) + [2\alpha + \gamma]T\,\lambda(T). \tag{3}$$

The diffusion thermopower is given by the well known relation [19]

$$S_D(T) = -\frac{\pi^2 k_B^2}{3|e|E_F}\xi_D T \qquad \text{with} \qquad \xi_D = \left.\frac{\partial \ln \sigma(E)}{\partial E}\right|_{E=E_F} \tag{4}$$

using standard notation. The sign of ξ_D determines the sign of S_D. In the free-electron model ξ_D is a positive constant giving $S_D(T)/T < 0$ and temperature independent—see e.g. [20].

According to equation (3) the thermopower can be described by the sum of two terms. The first term reflects in first approximation the mass-enhancement factor $[1 + \lambda(T)]$ due to many-body effects in a rather well known form. The second term is due to the renormalization of the electron velocity and relaxation time (2α) and to higher-order diagrams (γ) [18]. While the enhancement factor $[1 + \lambda(T)]$ is always positive, the factor $[2\alpha + \gamma]$ could have either sign [18] and therefore the second term can overcompensate the first one, giving rise to a dip in $S(T)$. The temperature dependence of the enhancement function $\lambda(T)$ was calculated in [21] and is given in a reduced representation as $\lambda(T)/\lambda(0)$

versus T/Θ^* [22]. Θ^* is an effective Debye temperature. $\lambda(T)$ decreases with increasing temperature and vanishes at temperatures well above Θ^*. Fine structures in $S(T)$ at low temperatures caused by fine structures in $\lambda(T)$ observed in amorphous CuZr samples [23] give strong evidence for the validity of equation (3). In our experiments these structures cannot be resolved.

In order to fit our data to equation (2) we assumed $S_D(T)/T$ and $[2\alpha + \gamma]$ to be temperature independent and calculated $\lambda(0)$ using McMillan's formula [24]. Besides $S_D(T)/T$ and $[2\alpha + \gamma]$ the fitting procedure yields Θ^*. Together with the measured superconducting transition temperature T_c in McMillan's formula, Θ^* was used instead of the Debye temperature Θ_D, which is unknown for amorphous Au_xSb_{100-x} films. It has been shown that Θ^* can differ significantly from Θ_D [25]. However $\lambda(0)$ does not change very much with Θ_D, since $\lambda(0)$ depends logarithmically on this quantity. The values of Θ^* of amorphous Au_xSb_{100-x} increase with increasing Au content from 100 K at 15 at.% to 160 K at 80 at.% with an uncertainity of approximately 30 to 50 %. More details of the fitting procedure are described in [26].

The fitting procedure just mentioned could not be applied sucessfully to all the films investigated. For films with $x < 14$ at.% $S_D(T)/T$ always turns out to be temperature dependent. This result is not surprising because according to theoretical investigations [27] $S_D(T)/T$ is expected to be temperature dependent near the MI transition. On the other hand close to the MI transition $S_D(T)$ is very much larger than $S_{add}(T)$ and therefore $S_D(T)$ could be approximated very well by $S(T)$.

For completeness, the concentration dependence of $[2\alpha + \gamma]$ is shown in figure 7 for the films investigated in this paper together with corresponding values of amorphous AuSn and AgIn [26]. Obviously the three amorphous alloys behave in a very similar way with respect to $[2\alpha + \gamma]$. The alloys with low noble-metal content especially have nearly the same value of $[2\alpha + \gamma]$. This is interesting because amorphous AuSn and AgIn in contrast to amorphous AuSb do not show a MI transition. The large negative values of $[2\alpha + \gamma]$ around 20 at.% noble metal are responsible for the negative sign of $S(T)/T|_{T\to 0}$ which is observed between 16.8 at.% and 37 at.% Au as shown in figure 6.

Finally, we want to discuss the behaviour of $S_D(T)/T|_{T\to 0}$ when x approaches x_c in the metallic region, which should diverge according to different theoretical investigations. Sivan *et al* [27] and Castellani *et al* [28] have calculated the energy dependence of the diffusion thermopower in the metallic regime. Approaching the MI transition these calculations give $S_D(T)/T|_{T\to 0} \propto (E_F - E_c)^{-\mu}$, with $E_F > E_c$ where E_F is the Fermi energy and E_c the mobility edge, which separates localized electron states from delocalized ones. The critical exponent μ depends, e.g., on the influence of the electron–electron interaction. If the electron–electron interaction can be neglected, then $\mu = 1$ [28]. Under the same condition $\sigma(E)$ vanishes with a critical exponent $\nu = 1$ [14]. In this case the electrical conductivity changes, to a first approximation, also linearly with concentration which has indeed been found in our experiments; see figure 2.

Combining the energy dependences of $S_D(T)/T|_{T\to 0}$ and $\sigma(E)$ found in the scaling approach gives

$$\left.\frac{S_D(T)}{T}\right|_{T\to 0} = \text{constant} \times \rho(T \to 0) \qquad \text{for } x > x_c. \tag{5}$$

This is the same relation as one obtains using Mott's expression for the diffusion thermopower (equation (4)) and the scaling behaviour of $\sigma(E)$. To check the validity of equation (5) we have plotted our data for 9 at.% $\leqslant x \leqslant$ 16.8 at.% in figure 8 in the appropriate way. The data for the films with $x < 14.2$ at.% are taken as measured, while for

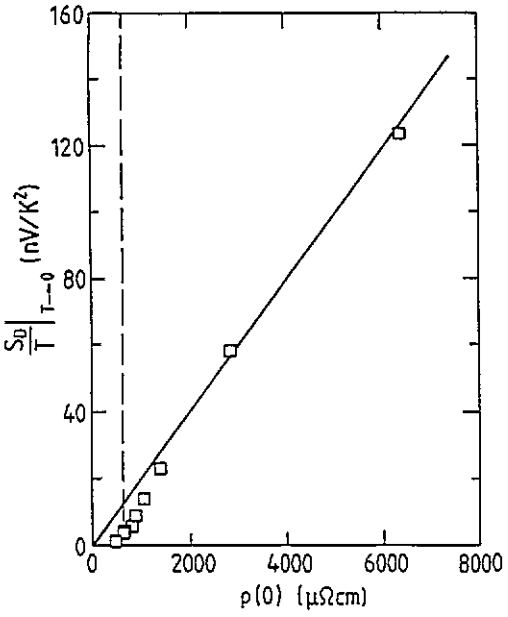

Figure 8. Low-temperature slope of S or S_D versus $\rho(0)$ for amorphous Au_xSb_{100-x}. For samples with $9 \leqslant x \leqslant 14.2$ at.% the values of $S(T)/T|_{T\to 0}$ are shown, while for samples with $x > 14.2$ at.% the values of $S_D(T)/T|_{T\to 0}$ taken from the fitting procedure are shown. All data were measured after annealing at 60 K. The solid line is a fit according to equation (5). The dashed line corresponds to the resistivity of a sample with $x = 14.2$ at.%.

higher Au concentrations $S_D(T)/T$ is taken from the fitting procedure as described above. At high resistivities, i.e. for small x, the relation is fulfilled quite well. The deviations at low resistivities may be caused by either of two factors. Firstly, x may be too far away from x_c. Secondly, putting $S(T)/T|_{T\to 0}$ instead of $S_D(T)/T|_{T\to 0}$ as was done for the films with $x < 14.2$ at.% results in values that are too small.

Although our experimental set-up was designed for thermopower measurements of metallic samples, we were able to measure $S(T)$ for an amorphous $Au_{7.5}Sb_{92.5}$ film which showed variable-range hopping conductivity below 25 K. For completeness and in order to show the behaviour of a non-metallic sample, $S(T)$ for this film measured after annealing at 60 K is given in figure 9. The temperature dependence of S is clearly non-linear and looks similar to that of the metallic film with $x = 9.0$ at.% which is shown for comparison in the same figure. In contrast to $S(T)$ of the metallic film, that of the $Au_{7.5}Sb_{92.5}$ film does not extrapolate to zero at low-temperatures. For this reason it is not possible to fit the low temperature data to $S(T) \propto T^n$ with $n = 1/2$ [29] or $n = 1/4$ [30, 31]. These relations are expected according to theoretical investigations which consider the contributions of variable-range hopping processes to the thermopower.

To get further information about the MI transition one of us (CL) intends to extend the experimental investigations of the thermopower and the electrical conductivity of amorphous films to temperatures well below 1 K and to concentrations closer to the transition.

4. Conclusions

From our investigation of the electrical conductivity and the thermopower of amorphous Au_xSb_{100-x} films we conclude that these films show a MI transition of the Anderson type. Approaching the transition from the metallic region, both the electrical resistivity and the low-temperature slope of the diffusion thermopower increase rapidly and depend linearly from each other. As far as we can see from our single measurement, corresponding investigations in the non-metallic region seem to be quite interesting. Finally the results

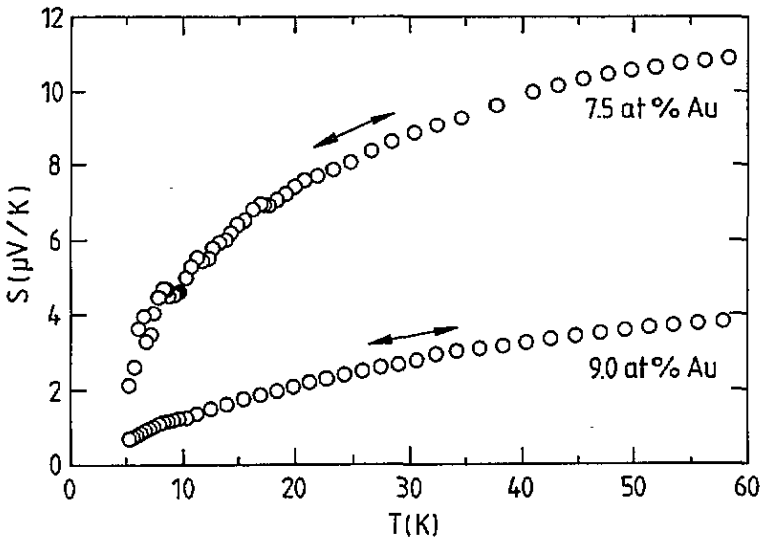

Figure 9. Temperature dependence of the thermopower S of a $Au_{7.5}Sb_{92.5}$ film ($x < x_c$) and of a Au_9Sb_{91} film ($x > x_c$).

of this investigation allow us to interpret recent experiments on Au/Sb sandwiches [7, 8]. The thermopower $S(T)$ of ultrathin Au films on top of amorphous Sb films as a function of increasing thickness of the Au film shows the same behaviour as that of amorphous Au_xSb_{100-x} films with increasing Au content.

Acknowledgments

We thank A B Kaiser, H von Löhneysen and T Moser for valuable discussions. Financial support from the Deutsche Forschungsgemeinschaft at the beginning of the investigation is gratefully acknowledged.

References

[1] Suhrmann R and Berndt W 1940 *Z. Phys.* **115** 17
[2] Richter H, Berckheimer H and Breitling G 1954 *Z. Naturf.* a **9** 236
[3] Hauser J J 1974 *Phys. Rev.* B **9** 2623
[4] Häussler P, Müller W H-G and Baumann F 1979 *Z. Phys.* B **35** 67
[5] Leitz H and Buckel W 1979 *Z. Phys.* B **35** 73
[6] Grasser H 1984 *Diploma Thesis* University of Karlsruhe
[7] Lauinger C and Baumann F 1994 *Physica* B **194–196** 1219
[8] Lauinger C, Boyen H-G and Baumann F 1995 to be published
[9] Roberts R 1977 *Phil. Mag.* **36** 91
[10] Compans E 1989 *Rev. Sci. Instrum.* **60** 2715
[11] Boyen H-G, Rieger P, Häussler P, Baumann F, Indlekofer G and Oelhafen P 1990 *J. Phys.: Condens. Matter* **2** 7115
[12] Stritzker B and Wühl H 1971 *Z. Phys.* **243** 361
[13] Hertel G, Bishop D J, Spencer E G, Rowell J M and Dynes R C 1983 *Phys. Rev. Lett.* **50** 743
[14] Lee P A and Ramakrishnan T V 1985 *Rev. Mod. Phys.* **57** 287
[15] Weitzel B, Schreyer A and Micklitz H 1990 *Europhys. Lett.* **12** 123
[16] Mott N F 1968 *J. Non-Cryst. Solids* **1** 1
[17] Kaiser A B 1984 *Phys. Rev.* B **29** 7088

[18] Kaiser A B and Stedman G E 1985 *Solid State Commun.* **54** 91
[19] Mott N F and Jones H 1936 *The Theory of the Properties of Metals and Alloys* (Oxford: Clarendon)
[20] Mahan G D 1990 *Many Particle Physics* (New York: Plenum)
[21] Kaiser A B 1982 *J. Phys.: F Met. Phys.* **12** L223
[22] Kaiser A B private communication
[23] Kaiser A B, Christie A L and Gallagher B L 1986 *Aust. J. Phys.* **39** 909
[24] McMillan W L 1968 *Phys. Rev.* **167** 331
[25] Bhatnagar A K, Pan R, Naugle D G and Kaiser A B 1990 *J. Phys.: Condens. Matter* **2** 6755
[26] Burkhardt M, Moser T, Compans E, Lauinger C, Loistl M and Baumann F 1992 *Solid State Commun.* **83** 655
[27] Sivan U and Imry Y 1986 *Phys. Rev.* B **33** 551
[28] Castellani C, Di Castro C, Gilli M and Strinati G 1988 *Phys. Rev.* B **37** 6663
[29] Zvyagin I P 1973 *Phys. Status Solidi* **58** 443
[30] Brenig W, Döhler G H and Wölfle P 1973 *Z. Phys.* **258** 381
[31] Kosarev V V 1975 *Sov. Phys.–Semicond.* **8** 897
[32] Mott N F and Davies E A 1979 *Electronic Processes in Non-Crystalline Materials* (Oxford: Clarendon)